A model of uniform cortical composition predicts the scaling laws of the mammalian cerebrum

Marc H.E. de Lussanet,[1,2*] Kim J. Boström,[1] Heiko Wagner[1,2]

[1]Movement Science, Westf. Wilhelms-Universität Münster
[2]Otto Creutzfeldt Center for Cognitive and Behavioral Neuroscience, Westf. Wilhelms-Universität Münster

[*]To whom correspondence should be addressed; E-mail: lussanet@uni-muenster.de.

The size of the mammalian cerebrum spans more than 5 orders of magnitude. The cortical surface gets increasingly folded and the proportion of white-to-gray matter volume increases with the total volume. These scaling relations have unusually little variation. Here, we develop a new theory of homogeneous composition of the cortex across mammals, validated with three simple numerical models. An extended tension model combined with a fractal-like growth rule, explains the pattern of gyri and sulci, as well as the arrangement of primary and secondary areas on the cortex. The second model predicts the white matter volume. The third model predicts the cortical surface area from the gray and white matter volume. All models have an $r^2 > 0.995$. Further, the last model accurately predicts the intraspecific variation for humans. Except for cetaceans, no clades show systematic deviations from the models, providing evidence that the regular architecture of the cortex shapes the cerebrum.

Introduction

Scaling relations are a classic field of evolutionary biology. The mammalian cerebrum ranges in size from about 10 mm^3 (pygmy shrew) to more than 5 dm^3 (fin whale (*1*)), i.e. more than 5 orders of magnitude. The scaling relations of the mammalian cerebrum are extraordinary because various parameters such as volume, surface, and proportion of gray matter all show trends with very little deviation across several orders of magnitude and independently of phylogenetic relationships (e.g. (*2, 3*)). This is in contrast to other scaling relations such as the encephalisation (expressed as brain-, cerebral- or cortical mass to body volume) which can vary by twentyfold between species of the the same body mass (*4*), and which have different scaling relations within species versus between species, and between phylogenetic groups (*4–6*).

The tight scaling relations suggest a simple scaling mechanism that depends on only a few parameters. It is tempting to assume isometric scaling in some form, but this is not the case (*7*). Understanding the common mechanisms that underlie the scaling relations will help to formulate scaling laws; to identify exceptions from these laws and thus help to understand evolutionary differences between species and brain regions (*8, 9*).

One remarkable scaling relation of the mammalian cerebrum exists between volume and total surface area (*10*). Under the assumption that the overall shape of the cerebrum is scale-independent (*11*), this relation is equivalent to the relation between exposed surface area and total surface area, which is sometimes expressed as a ratio (called folding index or cephalization index: (*5*)). A second remarkable scaling relation has been found between the volume of gray and white matter (*3*). More recently, a fractal-like relation between the total surface, the exposed surface, and the ratio of the volume to the exposed surface has been proposed (*12*). It was shown however, that this scaling relation amounts to the simpler assumption that the folding index times the proportion of gray matter volume is approximately constant (*13*).

It is widely accepted that the mammalian cerebral cortex shows a highly homogeneous composition of layers and neuronal cortical columns. The layers differ between regions of the mature cortex, but always show the developmental state of six layers at some time (*14*). Cortical columns integrate the layers perpendicularly to the cortical surface, and are regarded as computational units, which are highly uniform across the size range of the cerebrum (*15*). It is thought that the volume of cortical columns is independent of the local curvature of the cortical surface (*16*). Evidence from precise counting studies across species suggest that the number of cortical neurons per square millimeter is invariably close to $\sim 10^5$ per mm^2 (*17, 18*).

According to the cortical surface to volume scaling relation, the total surface area of the cortex increases overproportionately with the volume of the cerebrum. Consequently, the cortex of small cerebrums (such as that of mice) have a smooth surface, which is called *lissencephalic*, whereas the cortex of large cerebrums (such as that of humans) is increasingly folded, which is called *gyrencephalic*. Van Essen (*19*) proposed that the developmental mechanism by which the cortical surface becomes so strongly curved involves the elastic tension exerted by axons. Accordingly, when strained due to cortical growth, axons would pull the cortical surface into a convex curvature, leading to the typical folding pattern. However, on the basis of numerical simulations and dynamic tensor imaging (DTI) it has been questioned if, indeed, the axonal tension hypothesis can explain the convex curvatures of the gyri (*20*).

Here, we propose a new theory to explain the empirical scaling relations of the mammalian cerebrum. We derive simple mathematical scaling laws for the relations between cerebral volume and cortical surface area as well as for the volumetric relation of gray and white matter. The derived scaling laws are validated using three databases: a volumetric database across a wide range of mammals (*3*), a volume-surface database for human cerebrums (*21*), and a newly constructed volume-surface database for a wide range of mammals, which we composed from the existing literature.

The proposed theory is an extension of Van Essen's above mentioned tension hypothesis (*19*). It proceeds from the known fact that the growing immature cortex develops an alternating pattern of maturing and growth zones with long-range extra-cortical and short-range intra-cortical axonal connections, respectively. The maturing zones either receive sensory input or generate motor output, and respectively form the primary sensory and motor areas present in all mammals. As the cerebrum grows, so we hypothesize, the tension in the long-range axonal connections keeps the maturing zones from growing outwards and so they fold inwards and form sulci, while the growth zones between the maturing zones grow outwards and form gyri (Fig. 1). The width of the gyri is constrained by the height of the cortical columns and the relatively dense short-range connections. As the apex of a gyrus grows outward, it becomes wider, the flanks become separated, and another sulcus is formed (Fig. 2).

From the proposed extended tension model (ETM) it is possible to derive simple scaling laws for the above mentioned empirical scaling relations. We derive three scaling equations: The first one represents a first-order model that neglects the white matter volume. More specifically, it is a two-dimensional (2D) growth model, according to which the gyri branch as soon as they exceed a critical width. Already this simple model predicts the empirical data very well.

The second model yields an equation for the white matter volume on the basis of the extended tension model, and will be validated with the dataset of Zhang & Sejnowski (*3*).

The third model yields an equation for the gray and white matter volume and the total cortical surface area on the basis of the previous models. Since no data exist that combine estimates of the cortical surface as well as of the gray and white matter volumes, the model will be validated using our newly constructed database, as well as the human dataset of Toro et al. (*21*), assuming that the second model is correct.

According to our view, the regular scaling relations of the cerebrum do not reflect an evolutionary optimum. Rather, we hypothesise that valid scaling laws can be formulated on the basis

a simple growth rule and the uniform structure of the cortical building blocks.

Modelling

First order model: Fractal-like growth rule for gyrification

The first of our three models neglects the white matter contribution to the cerebral volume. It is based on the central hypothesis of a homogeneous composition of the cortex. Accordingly, the thickness of the cortex is limited, so once the critical thickness is reached, growth is only possible if the cortex invaginates, to form a sulcus (Fig. 2). If the cerebrum exceeds a critical size (inner section "1" in Fig. 2), a sulcus is initiated, but as long as it is smaller than the critical size, its surface is smooth (lissencephalic).

According to the first model, growth only occurs on the apex of each gyrus, and so the valley of a sulcus, once formed, will not move away from the center. Thus, the number of sulci decreases linearly when moving from the surface to the center of the cerebrum.

Note, that for very small cerebrums, the surface is entirely on the outside, so the cortical surface A scales to the cerebral volume V according to an isometric scaling law: $A = cV$ (with c being a constant). On the other hand, for very large cerebrums, most of the cortical surface lies within the sulci, and since the thickness of the gyri remains constant, the surface will scale to the volume in a linear manner. Thus, the model will interpolate between the two scaling laws: a 2/3 power law for very small cerebrums and a linear scaling for very large ones (cf. Fig. 3).

Note that this simple, first order model is just two-dimensional (2D), which is sufficiently realistic, though, because primary fields are elongated, so that gyri and sulci are elongated as well.

Analytically, the total circumference C of the 2D model is the sum of the exposed and non-exposed (inward) circumferences, which can be calculated as: $C = (2\pi R) + (2\pi)/(d_{\text{crit}})R^2 - R)$ for a circle with radius R and straight sulci. Additionally, a shape constant can be introduced to

account for the deviation of an exact circular shape of the model, the 3D version of the model will thus be of the general form: $C = R^2/d + sR$, where d has the dimension of length and is related to the critical distance d_{crit}, and where s is a dimensionless shape parameter.

When adding the third dimension, the total circumference becomes the total cortical surface A. The exposed surface will scale with the volume V to the 2/3 power in analogy to the surface of a sphere, so $V \sim R^3$, whereas the non-exposed, inward folded surface scales again linearly with the volume (as a result of the invariant gyral thickness), so $V \sim A^{3/2}$. In summary, the 3D version of the model is of the general form $V = A^{3/2}/d + sA$, where d is, again, a thickness parameter with the dimension of length, and where s is a dimensionless shape parameter. Note that d and s in the 2D and 3D models are different but analogous parameters.

Model 2: gray and white matter volumes

White matter consists of myelinized long-distance axonal connections. To answer the question how the volume of the white matter relates to the gray matter it is, therefore, essential to know how the diameter of axonal connections depends on the length of the axons. For example, it is well known that the myelin sheath increases the signal transmission velocity linearly with the axonal radius (*22*). Many invertebrates possess a few giant axons for long-range startle responses. Accordingly, one might expect large mammalian cerebrums to have axons with a wide diameter.

However, since the axonal volume increases quadratically with its diameter, a bundle of many narrow axons will transmit more information per second than a bundle with the same cross-section, which consists of a few wide axons. Moreover, due to noise, the efficiency of information transfer decreases with the spike rate according to Shannon's information theory (*23*). Indeed, it has been estimated from the frog's retina that each cell type transmits approximately the same amount of information independent of its axonal diameter, so that thin fibres transmit

vastly more information per summed cross-sectional area than thick ones (*24*). Consistently, the axonal width distribution in the mammalian brain seems to be largely independent of brain size (*25*).

Given that the distribution of axonal diameters in the white matter is independent of brain size, the volume of the axonal connections increases linearly with the distance between the regions that they connect. The summed cross-section A_W of the axonal connections scales with the number of neurons in the gray matter, which in turn scales with the gray matter volume. It follows that the summed cross-section A_W scales with the gray matter volume. Since the white matter volume W is proportional to the mean axonal length $\bar{l}$ times the summed cross section A_W, we obtain

$$W = \bar{l} A_W \propto \bar{l} G. \tag{1}$$

Part of the axonal connections will be intra-gyral, so that their length is independent of the size of the cerebrum. On the other hand, the length of long-distance extra-gyral connections will scale with the radius R of the cerebrum. Given our central assumption that the compositional scheme of the cortex, as outlined above (Fig 1), is independent of the size of the brain, the proportion of short-distance and long-distance connections should be constant with respect to the cerebral radius R. Given the characteristic overall shape of the cerebrum, the total volume of the cerebrum will scale with the cube of R, so the cerebral volume obtains $V = cR^3$, with c being a shape constant. The white matter volume W is the sum of the local and global connections, and so we obtain

$$W = G\left(a\sqrt[3]{V/c} + b\right) \tag{2}$$

Replacing $W = V - G$ and $\hat{a} = a/\sqrt[3]{c}$ we obtain for the gray matter volume:

$$G = V/(\hat{a}\sqrt[3]{V} + b - 1) \tag{3}$$

Model 3: surface to volume

The available databases do not include measurements of both the white matter volume and the total cortical surface. But as we now have a model to estimate the gray and white matter volume from the total volume (cf. Model 2; Fig. 4), we go further and estimate the white matter volume on the basis of this model.

This model will result in two equations, one for convoluted or *gyrencephalic* cerebrums (Eq. (10)) and one for smooth or *lissencephalic* cerebrums (Eq. (11)).

The outer ("exposed") border of the cerebrum differs from the deeper parts: 1. it does not contain any white matter, only gray cortex; 2. it is formed of the apex of gyri, so that the cortex in this border region is more strongly curved than the cortex inside the sulci.

We can thus distinguish the cortex (with volume G) into a convex gyral border of volume G_B and thickness λ, and a more planar to concave sulcal core of volume G_C and a radius $R-\lambda$. Since the bottom of the sulcus occupies a very small part of the total cortical surface, it can be neglected and it follows that the area of the core surface obtains

$$A_C = G_C/\lambda. \tag{4}$$

The volume V_C of the core consists of gray and white matter, so we have $V_C = G_C + W$, with W from Equations (2) and (3). Simultaneously, the core volume is approximately equal to the volume of a ball of radius $R - \lambda$ (see above), so

$$V_C = 4/3\pi(R-\lambda)^3 = 4\pi\left(R^3/3 - R^2\lambda + R\lambda^2 - \lambda^3/3\right). \tag{5}$$

Using Eq. (4) and (5), the core surface area A_C can thus be expressed as

$$A_C = (V_C - W)/\lambda = 4\pi\left(R^3/(3\lambda) - R^2 + R\lambda - \lambda^2/3\right) - W/\lambda. \tag{6}$$

The cerebral border region V_B is free of white matter but composed entirely of the convex part of the gyri. Due to the convexity, the cortical columns are not column-shaped as in the

sulcal regions of the cortex, but rather pie-shaped. Assuming that the cortical columns in the convex regions have the same volume as those in the flat, sulcal regions, the cortical surface per cortical column should be about twice as large in the cerebral border region. For the cortical surface in the border region A_B that:

$$A_B = 2V_B/\lambda. \tag{7}$$

The border volume is the cerebral volume minus the core volume, hence $V_B = V - V_C$. Let us approximate the cortical volume V by the volume of a ball of radius R, hence neglecting the sphericity, so $V = 4/3\pi R^3$, and let us use Eq. (5) for the core volume V_C, we then arrive at

$$V_B = V - V_C = 4/3\pi R^3 - 4/3\pi(R-\lambda)^3, \tag{8}$$

Inserting the above expression for V_B into Eq. (7), we obtain

$$A_B = 4\pi\left(2R^2 - 2R\lambda + 2/3\lambda^2\right), \tag{9}$$

Using the above equation and Eq. (6), the total cortical surface of a gyrencephalic cerebrum reads

$$A_{\text{gyr}} = A_B + A_C = 4\pi\left(R^3/(3\lambda) + R^2 - R\lambda + \lambda^2/3\right) - W/\lambda \tag{10}$$

with $V = 4/3\pi R^3$ as explained above.

If the radius of the cerebrum is smaller than the thickness of the border, the cerebrum is smooth (lissencephalic). In that case, the cortical surface is given by spheric volume and surface relations ($V = 4/3\pi R^3$ and $A = 4\pi R^2$):

$$A_{\text{liss}} = (36\pi)^{1/3} s V^{2/3}, \tag{11}$$

with the dimensionless sphericity constant $s = 1.56$ to correct for the deviation from a perfect sphere of the cortical hemispheres (Fig. S1).

Results

Model 1. The simple, first-order model described the cortical surface to cerebral volume data remarkably well, given that the white matter volume is neglected (Fig. 3A). The best fit to the logarithmic data (N=47 species) resulted in $s_3 = 0.20$ and $d_3 = 5.96$ m ($r^2 = 0.996$). The residual showed a small but significant U trend (Fig. 3B).

Model 2. The gray and white matter volume model described the data even better, with the best-fitting parameter values $\hat{a} = 0.00811$, $b = 2.060$, $r_W^2 = 0.997$; $r_G^2 = 0.9997$. The resulting two relations are plotted in Figure 4A. The residuals (log units) were generally much smaller for gray then for white matter volume (Fig. 4B: gray slope: $P < .05$, curvature: $P < .01$; white curvature: $P < .05$).

Model 3. The enhanced model for the relation of cortical surface to cerebral volume has just one single free parameter λ, which describes the cortical thickness. Fitting this parameter to the averages per species (excluding the human MRI data) and using a mean sphericity of $s = 1.57$ (Fig. S1), resulted in $\lambda = 2.81$ mm (N=47, $r^2 = 0.996$; Fig. 5A). (Without the cetaceans, the fit would be even slightly better: $\lambda = 2.94$ mm, $r^2 = 0.997$.) The residuals (log units) are shown in Panel B (curvature: $P < .001$). The fitting of the individual measurements in the human dataset resulted in $\lambda = 2.97$ mm ($r^2 = 0.962$; Panel A-inset). The corresponding residual is shown in the inset, curvature: $P < .01$. For a part of the measurements (N=51 species) the exposed cerebral surface area was reported. Using σ, the cerebral volume was estimated for these measurements (Fig. 5C). The residuals (Panel D) systematically increase with cerebral volume ($P < .01$). Note, that the lissencephalic cerebrums are exactly on the predicted relation because cortical and exposed surface area are equal.

The ratio of estimated gray matter volume (obtained from model 2) to cortical surface area represents the effective cortical thickness (cf. (*13*)), and is shown in Fig. 6. The model (red

dashed curve) describes the general trend in the empirical data, but it displays considerable variation for gyrencephalic cerebrums.

Discussion

We have proposed a unified theoretical concept to explain the scaling relations of white matter volume and cerebral surface area. The basis of the concept is simple: the regular scaling patterns of the mammalian cerebrum are caused by, and reflect, the highly regular and uniform composition of the cortex into a fixed number of (six) layers and into a variable number of cortical columns. The three presented models are derived on the basis of these premises.

The first model explores the scaling property of a fractal growth rule for the gray matter volume. The notion that the cerebrum has a fractal-like morphology has been around for several decades (*12, 26, 27*), but could not be proven yet (*13*). Even though the growth model neglects the presence of white matter, it describes the scaling of the volume-surface relation already remarkably well (Fig. 3).

The mechanical mechanism that leads to cortical folding is an old question whose answer has been sought in differential growth (*28–30*). An important model proposed that the anisotropy of the orderly arrangement of white matter and the growth tension in axons might be a driving force to produce convex curvatures of the gyri (*19*). This model has been criticised because it does not predict a realistic folding pattern for the cortex (*20*).

Our addition to Van Essen's model includes the notion that axonal connections of primary regions will pull sulci, at first in primary regions. This new hypothesis, the Extended Tension Model (ETM) not only explains better why large cerebrums are folded, but it also predicts the hierarchical pattern of folding. It predicts that the deepest, first order sulci are also the most consistent ones across the size range. Lastly, it predicts that these primary sulci should coincide with the primary sensory and motor areas. Both of these predictions are indeed fulfilled:

the median fissure (olfaction), the calcarine sulcus (vision), the lateral sulcus (vestibular and audition), and the central sulcus (somatosensation and motor) are the deepest and most constant sulci across the mammalian cerebrum. The underlying assumption of the model is that the functional map of the mammalian cortex shows a uniform plan across the entire class, which is widely accepted (*31*).

The second, model derives the white matter volume by the additional assumption that the cross-section of white matter per gray matter volume is constant, and that a constant proportion of the white matter connections are connecting locally versus globally. With just two free parameters, the model fits the data well (r^2 equals 0.997 and 0.9997, respectively, see results). The small quadratic trend in the residual suggests that the model slightly overestimates the white matter volume in the smallest and the largest cerebrums. For small cerebrums this is indeed to be expected, when the radius of the cerebrum becomes smaller than the length of the local connections in a gyrencephalic cerebrum. For elephants and pilot whales (the two data points with the largest cerebrum $V \approx 2$ l) the model predicts the white matter volume to be larger than the gray matter volume which is not the case. Rather, the proportion of white matter seems to saturate around 45% for brains the size of humans and larger.

For comparison, Zhang & Sejnowski (*3*) proposed a model on the assumption that the cortical geometry minimizes the overall length of the axonal connections (maximizing compactness), predicting that $W \propto G^{4/3}$. The power of scaling is represented by the slope in a log-log graph. Linear regression on the log-log data resulted in a significantly lower slope of 1.23. By contrast, our model predicts the scaling power well, increasing slightly with cerebral size (from 1.09-1.36).

Model 3 contains just one single free parameter, the cortical thickness λ, while fitting the data really well ($r^2 = 0.996$). Across species the cortical thickness ($\lambda = 2.81$ mm) was very close to the intraspecific value for humans ($\lambda = 2.97$ mm). This latter value is within the

range reported by Bok for a single specimen (*16*). Our value for λ is somewhat higher than the *effective* cortical thickness (i.e., the ratio of $G/A = 2.63$ for humans, cf. Fig. 6; see also (*32*)). This is to be expected because the latter definition neglects that the cortical surface has a convoluted shape.

A chronic difficulty of earlier models has been to predict the power of the scaling relations for the cortical surface (*2, 7, 10, 12, 20*) as well as for the white matter volume (*3*). Hofman (*2*) found a slope of 0.83 for a linear regression on convoluted cerebrums. The current model predicts a power of scaling is very close to 0.83 within the size range of $10^4 - 10^7$ mm^3 and a slightly higher power for smaller sizes.

The reasoning underlying the present scaling theory is that across the huge size range, deviations from the general trend are small. It follows that few factors determine the general scaling pattern, so we derived analytic scaling relations. Obviously, this approach involves *simplifications*. For example, the number of neurons (*17, 18*) and the effective cortical thickness (*32*) are slightly different between the different lobes. However, since such local differences are present across species of different sizes (*17*), they will average out. Also, the cortical thickness λ depends on the curvedness (*16*). The model will therefore slightly overestimate the cortical surface area in the border region. On the other hand, it will slightly underestimate the cortical surface in the core region because the core region also contains gyri. Finally, the 3rd model assumes a spheric cerebrum. The central conclusion is, that, indeed, simple principles can be defined to predict almost the entire variation in white matter volume, cerebral surface area and folding pattern.

One might speculate about individual deviations (and the absence thereof) with respect to model 2 (see above) and 3. Remarkable is the absence of systematic effects of the literature despite the data being collected across an entire century using various methods (cf. supplementary Fig. S2B). One important source of error might be in the conservation artifacts (all studies

corrected for those artifacts). The small systematic differences in cortical surface area in human data from conserved specimen (*14, 33*) with respect to the in-vivo MRI data (*21*) might be due to the older age of the subjects in the earlier studies, which were analysed post mortem (Fig. 5A, inset). The overall slightly larger volume of Schlenska ((*34*), N=5) might be due to the small sample and the conservation artifacts. Given that the standard deviations in all four studies are very similar, suggests that the precision of the techniques used is good and relatively small in comparison to the natural variation in cerebral size.

Another remarkable pattern that phylogenetic trends are almost absent. The only clade that shows systematic deviations from the cortical surface model (no 3, Fig. 5A) are the cetaceans (*6, 35, 36*). Since the proportion of gray to white matter volume seems to be normal in cetaceans (Fig. 4A and ref. (*3*)), the data strongly suggest that cetaceans have an increased cortical surface area with respect to the entire cerebral volume, i.e., both the cortical thickness and the white matter volume are decreased with respect to the cortical surface area. For example the number of glia cells, e.g. astrocytes, throughout the cerebrum could be enhanced. Indeed, a large body of evidence shows that the large cerebrum cetaceans (and other aquatic mammals) does not provide them with superb cognition or intelligence, a lack of neuronal specialization and prefrontal cortex (*5, 37, 38*). Rather, the increased brain size seems to reflect a physiological specialisation. Manger et al. (*5*) argued that this physiological specialisation is heat production: the mammalian is highly sensitive to minor changes in temperature, so keeping brain warm in cold water should indeed present a major evolutionary pressure.

Humans, on the other hand, are remarkably close to the model fit, both for the 2nd and 3rd model. This finding is in line with earlier conclusions (*39, 40*). The data of Toro et al. (*21*) show, moreover, that the model predicts the scaling relation even within the human species well for young adult humans (Fig. 5A-B). The MRI data of prematurely born infants (*41*) suggests that the predicted scaling relation is reached around the age of normal gestation time (38-42 weeks:

Fig. S3). According to these data, the cerebrum is lissencephalic until about 10^5 mm, i.e., 50 times the transition to gyrencephaly in adult mammals (supplementary Figure S3). These data thus suggest, that the scaling relation is accurately predicted across the developmental span for humans post gestation.

A considerable number of models have been proposed to explain the cortical folding and the scaling relations of the mammalian cerebrum. Most have not been validated to empirical data (*2, 10, 19, 29, 30, 42–47*). Others were validated (*3, 7, 12, 20*), but failed to explain the empirical data. This state of research is confusing, given that the empirical data show such an unusually clear pattern, which suggests that the scaling relations are governed by just few parameters.

We have here proposed a model that explains the pattern of cerebral folding (gyrification), based on homogeneous construction principles. According to the principles, both white matter volume and cortical surface area are simple geometric scaling functions of the gray matter volume. The validation to the available empirical data shows that model and data are fully consistent.

Conclusions

1. Very few simple principles can be defined to predict almost the entire variation in white matter volume, cerebral surface area and folding pattern.

2. Our model is validated by the available empirical data.

3. Our new theory provides strong evidence that uniform cortical composition in mammals drives the most important scaling relations known from the literature.

4. We provide evidence that the cortical surface area and the volume of white matter in the mammalian cortex are governed by the volume of gray matter, probably due the cortex

being universally composed of cortical columns and being layered.

5. We propose an extended tension model (ETM) that explains the general pattern of sulci and why this pattern follows the cortical functional map.

6. The ETM also predicts a fractal-like growth rule and hierarchical patterning of the sulci.

7. The proposed scaling relation is largely independent of phylogenetic relations and even holds within the human species.

References

1. G. Pilleri, M. Gihr, *Investigations on Cetacea* **2**, 89 (1970).

2. M. A. Hofman, *Prog. Neurobiol.* **32**, 137 (1989).

3. K. Zhang, T. J. Sejnowski, *Proc. Natl. Acad. Sci. USA* **97**, 5621 (2000).

4. A. M. Boddy, *et al.*, *J. Evol. Biol.* **25**, 981 (2012).

5. P. R. Manger, *Biol. Rev.* **81**, 293 (2006).

6. P. R. Manger, M. Prowse, M. Haagensen, J. Hemingway, *J. Comp. Neurol.* **520**, 2430 (2012).

7. V. Braitenberg, *J. Comput. Neurosci.* **10**, 71 (2001).

8. P. Rakic, *Nature Reviews Neuroscience* **10**, 724 (2009).

9. D. C. Van Essen, *et al.*, *Proc. Natl. Acad. Sci. USA* **116**, 26173 (2019).

10. M. A. Hofman, *Brain Behav. Evol.* **27**, 28 (1985).

11. M. H. E. de Lussanet, *PeerJ PrePrints* **3**, e1518 (2015).

12. B. Mota, S. Herculano-Houzel, *Science* **349**, 74 (2015).

13. M. H. E. de Lussanet, *Science* **351**, 825 (2016).

14. K. Brodmann, *Verhandlungen der Gesellschaft Deutscher Naturforscher und Ärzte* **85**, 200 (1913).

15. P. Rakic, *Trends Neurosci.* **18**, 383 (1995).

16. S. T. Bok, *Zeitschr. gesamte Neur. Psych.* **121**, 682 (1929).

17. A. J. Rockel, R. W. Hiorns, T. P. S. Powell, *Brain* **103**, 221 (1980).

18. C. N. Carlo, C. F. Stevens, *Proc. Natl. Acad. Sci. USA* **110**, 1488 (2013).

19. D. C. Van Essen, *Nature* **385**, 313 (1997).

20. G. Xu, *et al.*, *J. Biomech. Eng.* **132**, 071013 (2010).

21. R. Toro, *et al.*, *Cereb. Cortex* **18**, 2352 (2008).

22. J. A. Perge, K. Koch, R. Miller, P. Sterling, V. Balasubramanian, *J. Neurosci.* **29**, 7917 (2009).

23. V. Balasubramanian, D. Kimber, M. J. Berry, *Neural Comput.* **13**, 799 (2001).

24. K. Koch, *et al.*, *Curr. Biol.* **16**, 1428 (2006).

25. J. A. Perge, J. E. Niven, E. Mugnaini, V. Balasubramanian, P. Sterling, *J. Neurosci.* **32**, 626 (2012).

26. M. A. Hofman, *J. Hirnforsch.* **32**, 103 (1991).

27. R. L. Stoop, V. Saase, C. Wagner, B. Stoop, R. Stoop, *Phys. Rev. Lett.* **110**, 108105 (2013).

28. G. F. Striedter, S. Srinivasan, E. S. Monuki, *Ann. Rev. Neurosci.* **38**, 291 (2015).

29. W. Le Gros Clark, *Essays on growth and form* (Oxford University Press, Oxford, 1945), pp. 1–22.

30. L. da Costa Campos, R. Hornung, G. Gompper, J. Elgeti, S. Caspers, *bioRxiv* **04**, 020172 (2020).

31. J. H. Kaas, *Brain Behav. Evol.* **78**, 7 (2011).

32. S. Frangou, *et al.*, *bioRxiv* (2020).

33. H. Elias, D. Schwartz, *Z. Säugetierk.* **36**, 147 (1971).

34. G. Schlenska, *Z. Anat. Entwickl. Gesch.* **128**, 47 (1969).

35. G. Roth, *Philosophical Transactions of the Royal Society of London B: Biological Sciences* **370**, 49 (2015).

36. L. Marino, *et al.*, *PLoS Biol.* **5**, 966 (2007).

37. P. R. Manger, *Neuroscience* **250**, 664 (2013).

38. N. Patzke, *et al.*, *Brain Struct. Funct.* **220**, 361 (2015).

39. F. A. C. Azevedo, *et al.*, *J. Comp. Neurol.* **513**, 532 (2009).

40. S. Herculano-Houzel, *Proc. Natl. Acad. Sci. USA* **109**, 10661 (2012).

41. O. Kapellou, *et al.*, *PLOS Medicine* **3**, 1 (2006).

42. J. Karbowski, *J. Comput. Neurosci.* **15**, 347 (2003).

43. G. Schlenska, *J. Hirnforsch.* **15**, 401 (1974).

44. H. J. Jerison, *Development and Evolution of Brain Size: Behavioral Implications*, C. J. M. E. Hahn, B. C. Dudek, eds. (Academic Press, New York, 1979), pp. 30–60.

45. J. W. Prothero, J. W. Sundsten, *Brain Behav. Evol.* **24**, 152 (1984).

46. P. H. Todd, *Journal of Theoretical Biology* **97**, 529 (1982).

47. B. Mota, S. Herculano-Houzel, *Front. Neuroanat.* **6**, 3 (2012).

Figure Captions

Figure 1. Sketch of the proposed extended tension model (ETM) with regional growth zones. A. In the developing cortex, growth zones alternate with maturing zones. The latter possess more dense long-range axonal connections. B. When the cerebrum increases in size, tension in the long-range axonal connections will restrain outward movement of matured zones. C. Consequently, the matured zones form sulci. The width of the gyri is restrained by the tension in the short-range connections between the cortex on the neighboring flanks.

Figure 2. Schematic pie-section of the first order model: The cortical surface (thick black curve) is on the exposed outside as well as in the sulci. As the cerebrum grows, the width of gyri will generally increase. If the width exceeds the critical width (d_{crit}), a new sulcus is formed. By this rule, the number of sulci, N, increases with the radius of the cerebrum. Note, that a small cerebrum with not have any sulci and will thus be lissencephalic (smooth).

Figure 3. First-order model fit to the data, on a logarithmic scale. Each dot represents the mean of one species (human data are in addition shown as a cloud). On a logarithmic scale, the model approaches two asymptotes: $A = 7.1V^{2/3}$ (isometric scaling relation), $A = 0.22V$ (linear relation). Blue and red shades: influence of 1 standard deviation for each of the two fitting parameters.

Figure 4. Model for gray and white matter volumes, fitted to the dataset of (*3*). According to Model 2 (Eq. (3)), the white matter volume scales to the cerebral size in two ways: long-range extra-gyral connections scale with the cerebral radius, and short-range, intra-gyral connections scale with the total cerebral surface. A. The fitted relation on a log-log scale, where the gray matter volume follows from the white matter volume ($V = W + G$). B. The residual on a log scale as a function of the cerebral volume. Note, that the residual has log-units. Black curves: linear and quadratic regressions to the white matter residual; purple curves: the same for the gray matter.

Figure 5. Results of model 3 for the cortical surface in relation to the cerebral volume. A. Gyrencephalic cerebrums scale with Eq. (10) (dashed curve); lissencephalic cerebrums scale with Eq. (11) (dash-dotted curve). Shaded regions show a factor 1.5 for the sphericity, s (blue) and cortical thickness λ (red) parameters. Note that the set of human MRI data (cloud of dots), was not included for the data fitting. Inset: The human data by literature source. B. The residual on log scale as a function of the cerebral volume. Black lane and lilac curve: linear and quadratic regression, respectively (including the cetaceans, blue dots). The inset shows the

human MRI data with the same vertical scale. C. The same model, for which exposed surface data was available, while estimating the cerebral volume from the exposed surface area (see methods). The black curves are the same as in Panel A. The red dashed curve shows the model fitted to just the cetaceans. D. The residual for panel D. Note, that the exposed surface equals cortical surface for lissencephalic cerebrums. The cetaceans are shown with blue dots.

Figure 6. The ratio of gray volume to cortical surface area G/A as a function of the cerebral volume ($\log(V)$). Vertical line: transition to convoluted cerebrums. Dashed curve: Prediction from Model 2 and 3.

Figures

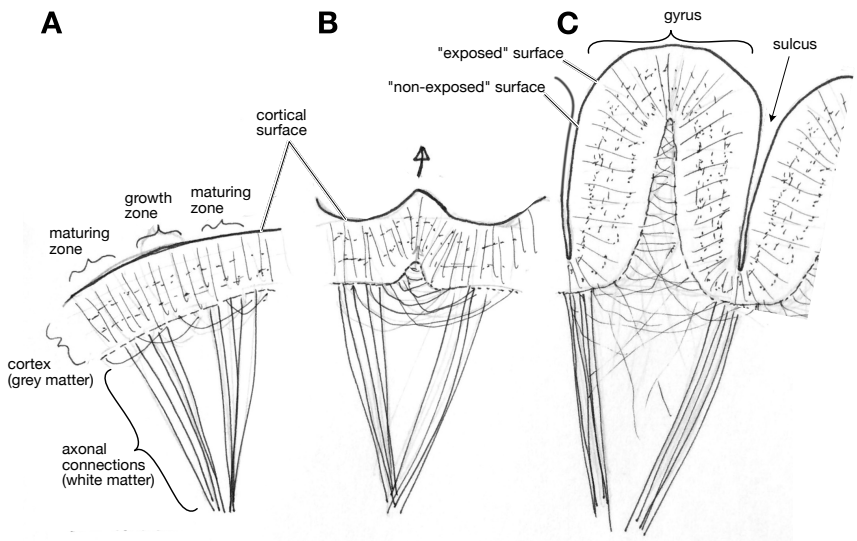

Figure 1: Sketch of the proposed extended tension model (ETM) with regional growth zones. A. In the developing cortex, growth zones alternate with maturing zones. The latter possess more dense long-range axonal connections. B. When the cerebrum increases in size, tension in the long-range axonal connections will restrain outward movement of matured zones. C. Consequently, the matured zones form sulci. The width of the gyri is restrained by the tension in the short-range connections between the cortex on the neighboring flanks.

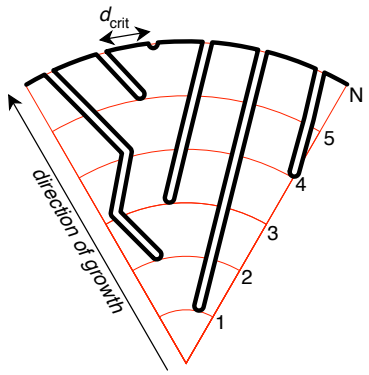

Figure 2: Schematic pie-section of the first order model: The cortical surface (thick black curve) is on the exposed outside as well as in the sulci. As the cerebrum grows, the width of gyri will generally increase. If the width exceeds the critical width (d_{crit}), a new sulcus is formed. By this rule, the number of sulci, N, increases with the radius of the cerebrum. Note, that a small cerebrum with not have any sulci and will thus be lissencephalic (smooth).

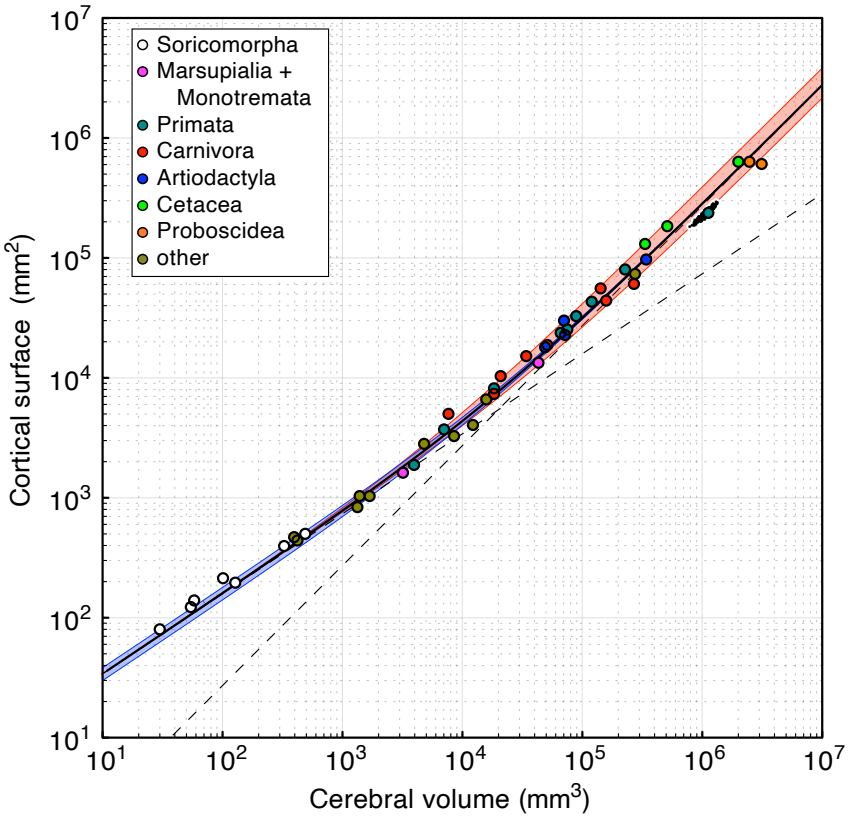

Figure 3: First-order model fit to the data, on a logarithmic scale. Each dot represents the mean of one species (human data are in addition shown as a cloud). On a logarithmic scale, the model approaches two asymptotes: $A = 7.1V^{2/3}$ (isometric scaling relation), $A = 0.22V$ (linear relation). Blue and red shades: influence of 1 standard deviation for each of the two fitting parameters.

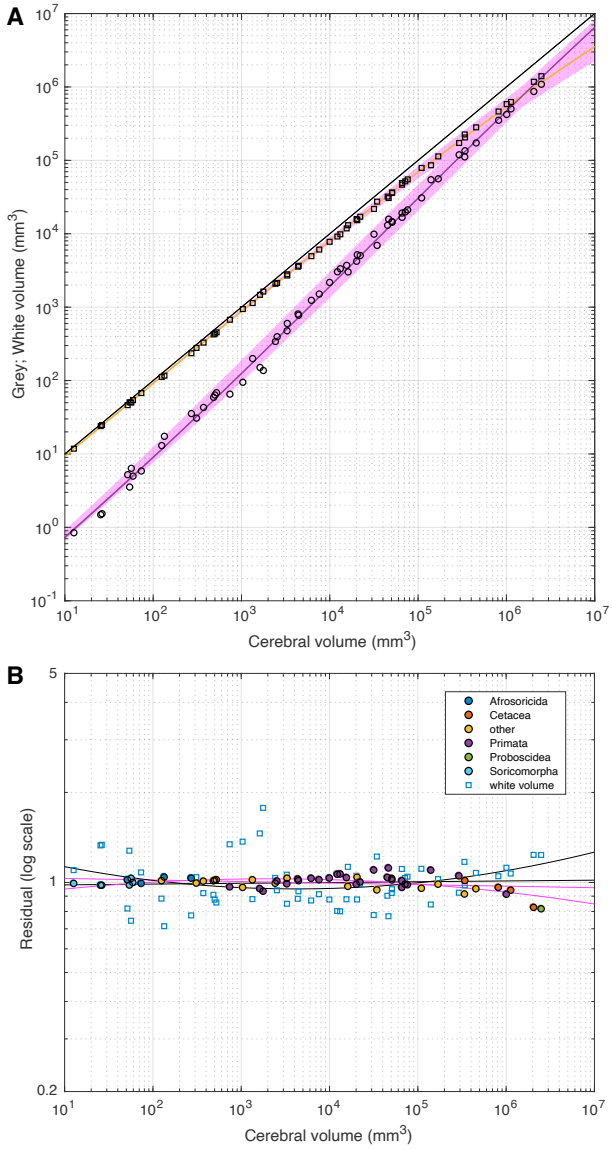

Figure 4: Model for gray and white matter volumes, fitted to the dataset of (*3*). According to Model 2 (Eq. (3)), the white matter volume scales to the cerebral size in two ways: long-range extra-gyral connections scale with the cerebral radius, and short-range, intra-gyral connections scale with the total cerebral surface. A. The fitted relation on a log-log scale, where the gray matter volume follows from the white matter volume ($V = W + G$). B. The residual on a log scale as a function of the cerebral volume. Note, that the residual has log-units. Black curves: linear and quadratic regressions to the white matter residual; purple curves: the same for the gray matter.

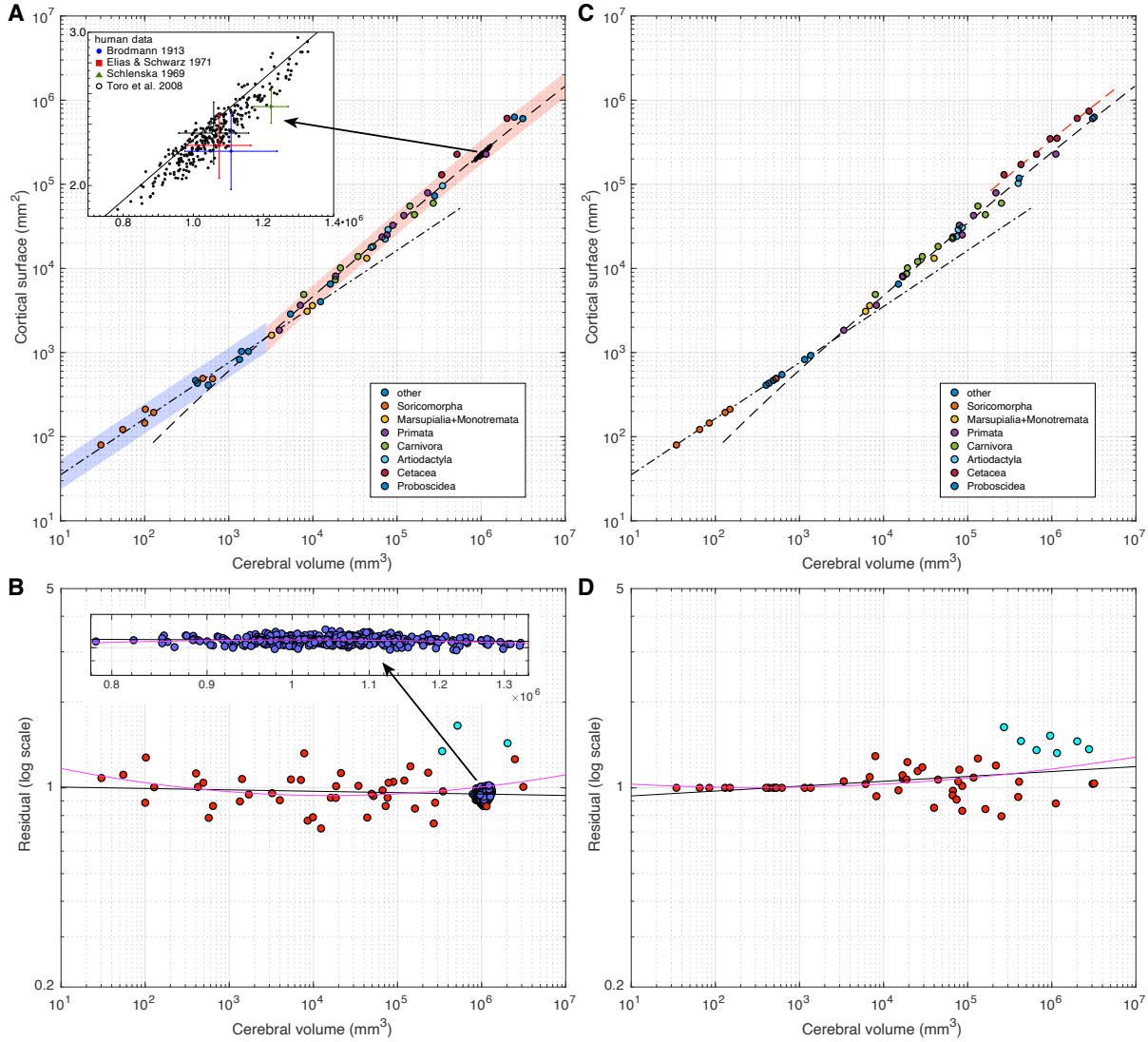

Figure 5: Results of model 3 for the cortical surface in relation to the cerebral volume. A. Gyrencephalic cerebrums scale with Eq. (10) (dashed curve); lissencephalic cerebrums scale with Eq. (11) (dash-dotted curve). Shaded regions show a factor 1.5 for the sphericity, s (blue) and cortical thickness λ (red) parameters. Note that the set of human MRI data (cloud of dots), was not included for the data fitting. Inset: The human data by literature source. B. The residual on log scale as a function of the cerebral volume. Black lane and lilac curve: linear and quadratic regression, respectively (including the cetaceans, blue dots). The inset shows the human MRI data with the same vertical scale. C. The same model, for which exposed surface data was available, while estimating the cerebral volume from the exposed surface area (see methods). The black curves are the same as in Panel A. The red dashed curve shows the model fitted to just the cetaceans. D. The residual for panel D. Note, that the exposed surface equals cortical surface for lissencephalic cerebrums. The cetaceans are shown with blue dots.

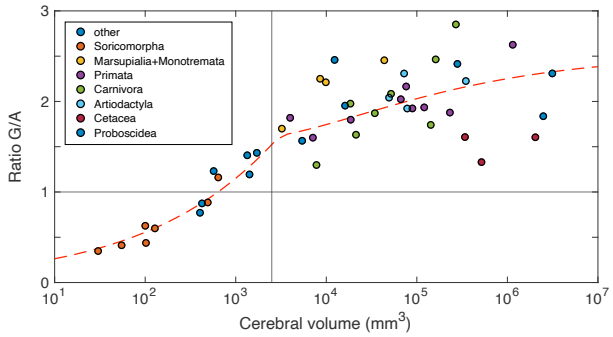

Figure 6: The ratio of gray volume to cortical surface area G/A as a function of the cerebral volume ($\log(V)$). Vertical line: transition to convoluted cerebrums. Dashed curve: Prediction from Model 2 and 3.